Journal of Applied Polymer SCIENCE

Ultraviolet–ozone surface cleaning of injection-molded, thermoplastic microcantilevers

Prabitha Urwyler,[1,2,3] Alfons Pascual,[4] Bert Müller,[1] Helmut Schift[2,5]

[1]Biomaterials Science Center, c/o University Hospital, University of Basel, 4031 Basel, Switzerland
[2]Laboratory for Micro- and Nanotechnology, Paul Scherrer Institut, 5232 Villigen PSI, Switzerland
[3]Gerontechnology and Rehabilitation Group, University of Bern, 3010 Bern, Switzerland
[4]Institute of Polymer Engineering, University of Applied Sciences (UAS) Northwestern Switzerland, 5210 Windisch, Switzerland
[5]Institute of Polymer Nanotechnology, UAS Northwestern Switzerland, 5210 Windisch, Switzerland
Correspondence to: H. Schift (E-mail: helmut.schift@psi.ch)

ABSTRACT: Ultraviolet–ozone (UVO) is used for the cleaning of labware from organic contamination and includes sterilization, surface roughening, and activation. A range of polymers has been treated without major effects on surface topography and surface chemistry. Even for those, which are subject to physical and chemical aging, a trade-off between damages and surface cleaning was often found. This communication presents a comprehensive overview on how to UVO-treat selected polymers known from applications in biology and medicine, in particular microcantilevers used for biosensing. The study provides well-defined thresholds below which degradation and surface damages are avoided. The impact of UVO treatments on the surface and bulk properties of the injection-molded polymers was examined by means of differential scanning calorimetry and Fourier transform infrared spectroscopy measurements. © 2015 Wiley Periodicals, Inc. J. Appl. Polym. Sci. **2015**, *132*, 41922.

INTRODUCTION

Various wet and dry processes have been developed for cleaning polymer labware from organic contamination.[1–3] Ultraviolet–ozone (UVO) treatments have been established because of easy use under ambient conditions.[4,5] Polymer materials have attracted great interest in bioanalytical applications owing to their light weight, low cost, and optical transparency. They offer tailored physical and chemical properties to be combined with low-cost production including injection molding. Therefore, polymers attracted more attention for applications in biosensors. Compared to silicon-based microcantilevers (μC), polymeric μC can exhibit better biocompatibility and much better adaptability of rapid prototyping along with mechanical properties, which make them particularly sensitive.[6] The sensitivity of the μC depends on the mechanical properties, i.e., the Young's modulus E and the Poisson ratio of the relevant material or composition. The advantage of injection molding for μC fabrication is that the polymer can be chosen so that the mechanical properties of the cantilever sensor are suitably adapted to the desired application. The UVO cleaning of injection-molded polypropylene (PP) μC was reported in detail.[7] The mechanism behind UVO cleaning is the photo-sensitized oxidation process,

in which the contaminant molecules are dissociated as the result of UV absorption.[8] Here, the hydrocarbons are converted into volatile compounds that desorb from the polymer surface by oxidation (see Figure 1).[8] This approach enables us to obtain ultra-clean surfaces free of organic contaminants. The cleaning processes usually damage the surface of the polymer in a significant manner. As UV light can also penetrate into the bulk of the polymer, the UVO application can modify the physical and chemical properties of the polymer, i.e., we observe phenomena such as chain scission and crosslinking.

The UVO treatment can significantly influence the structural properties of polymers. In the case of 50-μm-thin PP μCs the mechanical properties are affected.[7] A reasonable trade-off between the negative impact on the structure and the cleaning efficacy was found for UVO exposure times up to 20 min. This period of time is shorter than the 50-min standard protocol to treat silicon (Si) μC,[9] but long enough to ensure cleaning. UVO treatments as short as 10 min are insufficient to suitably remove the organic contaminations from polymer surfaces.[10] Longer treatment periods are intolerable as severe deterioration of the μC bending and surface characteristics takes place. Nanometer-thin gold coatings, often deposited to obtain reasonable laser
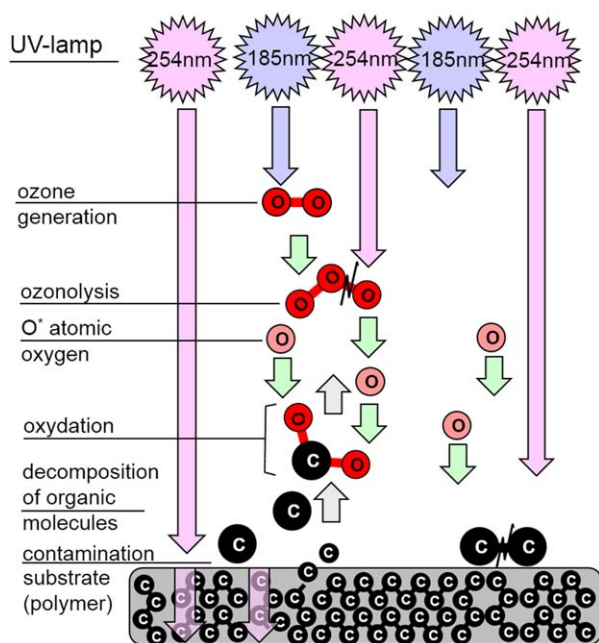
Figure 1. The UV–ozone cleaning process is a photosensitized oxidation process, in which the hydrocarbons are excited and/or dissociated owing to absorption of the UV radiation at the wavelengths of 184.7 and 253.9 nm. Although the UV light can penetrate into the bulk of the polymer and modify its structure, the oxidation is restricted to the surface region.[8] [Color figure can be viewed in the online issue, which is available at wileyonlinelibrary.com.]

beam reflectivity,[11] do not prevent the μC degradation, but cause a moderate retardation of the UVO-induced property modification. They also reduce the roughening of the surface, because the gold coating inhibits the dissolution of low-molecular-weight compounds generated during chain scission. Because of the correlation of the results from polymer analysis, i.e., differential scanning calorimetry (DSC), Fourier transform infrared (FTIR) spectroscopy, mechanical indentation, and bending experiments, a threshold could be defined from a single method. Each of the techniques enables to define a tolerable maximum cleaning time (see Figure 2). For PP μC, the UVO treatment induces chemical aging without any delay, i.e., no dwell time was detectable. The mechanical properties of the PP μC, however, remain constant for a reasonable period of UVO treatment. They correlate with enthalpy ΔH_c changes detected by means of DSC.[7] One cannot *a priori* assume a comparable behavior for other medically relevant polymers, as the degradation mechanisms are material-dependent. The question arises how far the results obtained for PP μC correspond to other polymers regularly applied for biosensing, microfluidics, and load-bearing implants.

EXPERIMENTAL

Polymer Materials

Cyclic olefin copolymer (COC; Topas 8007x10, Topas Advanced Polymers GmbH, Frankfurt-Hoechst, Germany) is often part of microfluidic elements because of its comparably high glass transition temperature (T_g), limited moisture uptake, chemical resistance, and excellent optical properties. Polyoxymethylene
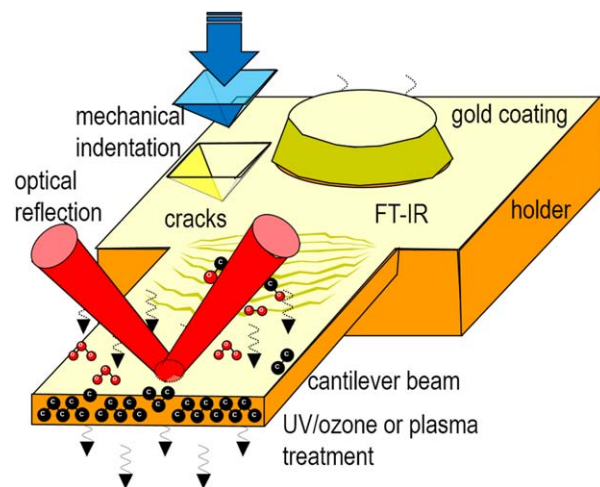
Figure 2. Schematic displaying experimental techniques to analyze the phenomena occurring during the cleaning of μCs using UVO: mechanical indentation, FTIR, DSC, SEM, and optical microscopy, and bending/deflection measurements using optical read-out. Typical thicknesses are 35–50 μm of the μC beam and 500 μm for the holder. [Color figure can be viewed in the online issue, which is available at wileyonlinelibrary.com.]

(POM; 511P Delrin NC010, Dupont, Le Grand Saconnex, Switzerland) is used in some esthetic orthodontic brackets and as acetabular components, whereas polyvinylidene fluoride (PVDF; Kynar 720, Arkema, Puteaux, France) in components of bioanalytical devices. The biodegradable polymer poly(lactic acid) (PLA; Resomer® LR 708, Boehringer Ingelheim GmbH, Ingelheim, Germany) is applied as absorbable suture, skin grafts, implants, and controlled drug delivery systems. The high-performance polyether ether ketone (PEEK; KetaSpire KT-880NT, Solvay Advanced Polymers, Cologne, Germany) is the main ingredient of load-bearing implants and pacemaker housings.

Preparation of μCs

The polymers COC, POM, PVDF, PLA, and PEEK were used to fabricate μC taking advantage of microinjection molding (μIM) and a modular μIM tool as described.[6,12] The molding tool was installed in an Arburg 320 Allrounder (Arburg, Lossburg, Germany) with a maximum clamping force of 600 kN. At the mirror unit of the molding tool a polished steel surface ensured an optically flat and smooth surface on one side of the μCs. The microcavities at the tool unit were generated by laser ablation. The μC array was designed with outlines of a micromachined 500-μm-thick Si μC array with a 3.5×2.5 mm^2 body (holder). It has eight 480 μm-long, 80–130 μm-wide, and 35–50 μm-thick μC beams. The injection molding process parameters for the polymers enclosed to this study were selected according to the information given in the datasheets of the related suppliers, and they are listed in Table I.[6,12]

UVO Surface Cleaning of COC, POM, PVDF, PLA, and PEEK μC

The flat mirror side of the μC surface was treated in a UVO cleaner (UV Clean Model 13550, Boekel Scientific, Feasterville,

Table I. Injection Molding Process Parameters as Set for the Polymers Used

Material/Parameters	PVDF	PEEK	COC	POM	PLA
Melting temperature (°C)	220	400	240	220	200
Tool temperature (°C)	120	225	77	120	40
Mold insert temperature (°C)	120	260	77	120	40
Injection speed (cm³/s)	10	10	30	10	10

PA) at ambient conditions. Batches of bare μCs were cleaned for periods ranging from 30 to 120 min.

Optical Microscopy

Surface inspection of UVO-treated μCs was carried out by means of optical microscopy (DMRX, Leica Microsystems GmbH, Jena, Germany). The pictures were taken with a multi-focusing software (ProgRes®CapturePro 2.7, JENOPTIK Optical Systems GmBH, Jena, Germany) to precisely record the irregular surfaces of the μCs after UVO exposure.

Fourier Transform Infrared Spectroscopy

Reflection FTIR spectra of two regions on the μC array, i.e., close to the μC fingers and holder, respectively, were recorded using a Centaurus IR-microscope coupled to a Nexus IR spectrometer (Thermo Electron Corporation, Thermo Fisher Scientific, Dreieich, Germany) with a grid of $300 \times 300\ \mu\text{m}^2$. Two μC arrays of non-UVO-treated specimens were measured as reference. The background spectra were recorded every 15 min.

Differential Scanning Calorimetry

For the thermal analysis, the μC arrays with a mass between 3 and 4 mg were sealed to an aluminum cup to acquire DSC (DSCQ1000, TA Instruments, Waters GmbH, Eschborn, Germany) data. The complete protocol, consisting of a first heating cycle from a temperature of 0 to 250°C, except 400°C for PEEK, subsequent cooling to 0°C, and a second heating cycle again to a temperature of 250°C, was conducted in a dry nitrogen atmosphere. The heating and cooling rates were set to 10 K/min.

RESULTS AND DISCUSSION

The impact of UVO cleaning is a process, which strongly depends on the chemical structure of the polymer and the thermal history of the injection-molded polymer sample. The morphology of the injection-molded polymeric μC strongly influences the sensitivity to degradation. Our results for POM and PP[7] support the findings that the amorphous skin layer, which results from rapid cooling on contact with the mold, is more prone to degradation than the crystalline bulk region of the polymeric μC.[13] For the semicrystalline polymer POM, optical microscopy images (cf. Figure 3) obtained from μC treated for a period of 2 h exhibit a microstructure with cracks. The orientation of these cracks does not represent the melt flow from injection molding, as observed for the PP μCs.[7] The morphology of the degraded POM surface shows a pattern that indicates generalized surface (and bulk) degradation through mass loss and cracking.[14] Owing to the molding process temperature of 120°C POM exhibits an increased crystallinity without further impact on the DSC behavior. The UVO surface cleaning leads to chemical decomposition of POM and results in an increasing formation of stress-induced cracks. This behavior indicates the preferential removal of amorphous POM with respect to the crystalline areas. It is noteworthy to mention that the morphology of the UVO-treated PP and POM reveals the polymer flow into the thin mold cavities.

Upon UVO exposure, the polymers show characteristic changes or remain mainly unchanged. The main chemical aging processes upon UVO exposure are thermo-oxidative degradation of the surface and hydrolytical degradation of the polymer chain. Oxidation usually occurs at the tertiary carbon atom present in every repeat unit. A free radical could be formed here which then reacts further with oxygen, followed by chain scission to yield aldehydes and carboxylic acids. Externally, this shows up
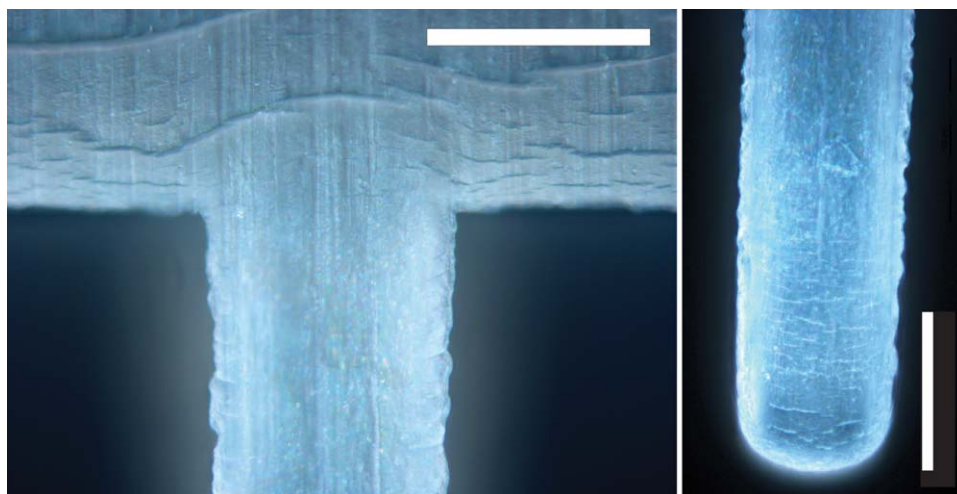
Figure 3. The optical micrographs from POM μCs UVO-treated for 120 min show the presence of cracks. The scale bars correspond to 100 μm. [Color figure can be viewed in the online issue, which is available at wileyonlinelibrary.com.]
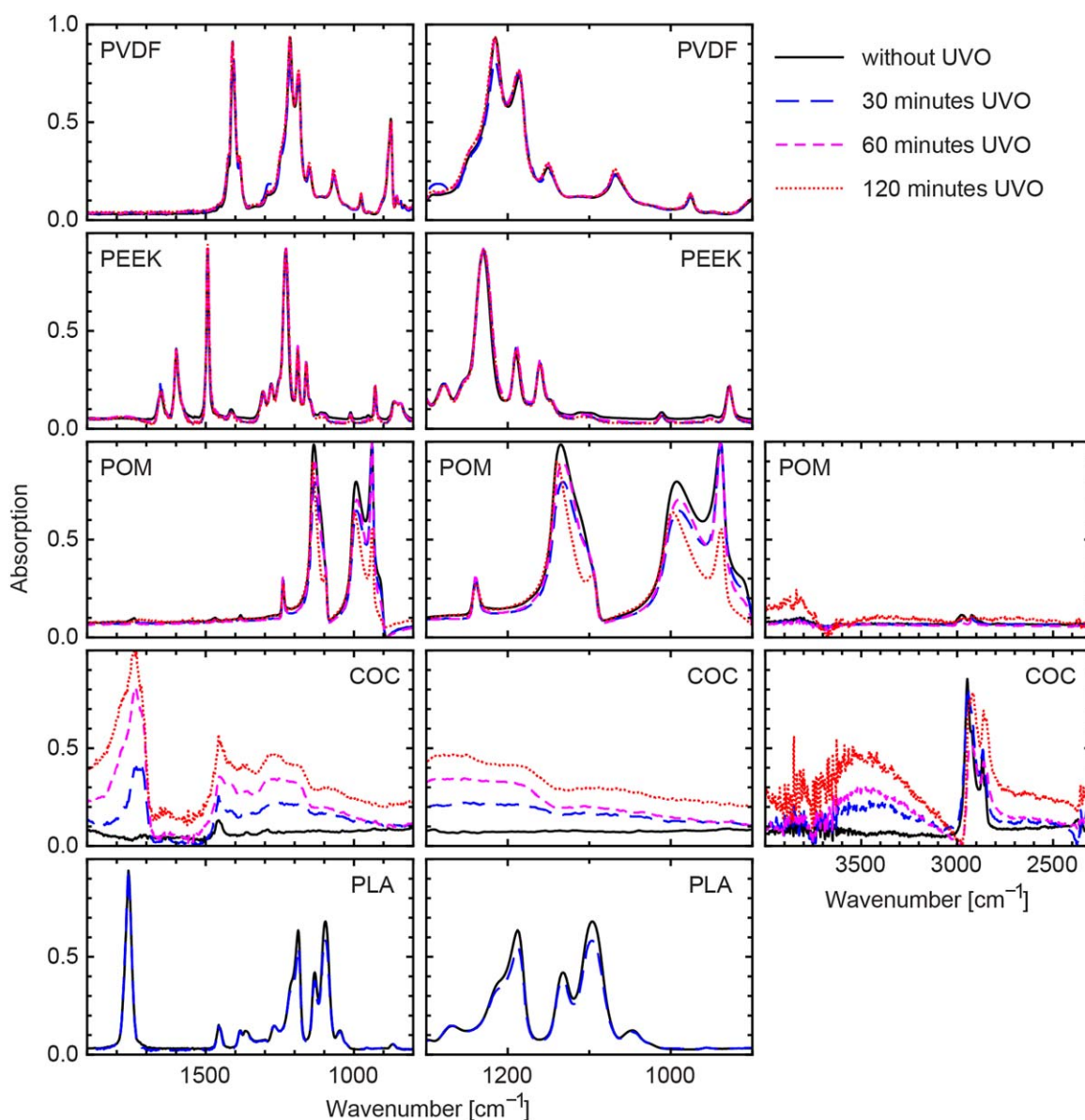
Figure 4. The FTIR spectra for PVDF, PEEK, POM, COC, and PLA obtained after a series of UVO exposure times (0 min, black solid line; 30 min, blue long-dashed line; 60 min, violet dashed line; 120 min, red dotted line) show relatively strong changes for COC, moderate changes for POM, and minor or no changes for PEEK, PVDF, and PLA. [Color figure can be viewed in the online issue, which is available at wileyonlinelibrary.com.]

as a network of fine cracks. They proceed growing deeper and become more severe with exposure time. This characteristic behavior is due to the thermomechanical stress generated in the surface layers.

Carbon–carbon double bonds (C═C) and carbonyl groups (C═O), which exist within the regular structure of the polymer, are capable of absorbing UV photons, which lead to photo-oxidative reactions and, finally, result in the degradation of the polymer. For PLA, the energy of the photons with a wavelength of 400 nm or shorter breaks down the covalent bonds of C─C and C─O and the ozone generated oxidizes the polymer surface. For polymers that have no carbonyl or C═C bonds within their regular structure, these moieties are introduced into the backbone or side groups through the high-

temperature injection molding process. It is known that oxygen and radiation are viable mechanisms for the chemical breakdown of POM.[15]

For characteristic thermoplastic polymers low-molecular-weight fragments are formed through chain scission, resulting in a reduced T_g.[16,17] For PP, the entire 50 μm-thick μC is affected owing to the UV transparency.[18] The polymers described here exhibit a significantly lower UV transparency and therefore absorb the light with wavelengths of 184.7 and 253.9 nm near the surface. To this end, the affected volume fraction of μC and holder is much smaller than for PP. The related changes in the DSC signal are, therefore, less prominent. Because of the transparency of COC to UV light, low-molecular-weight fragments are formed through chain scission.

Table II. Summarized Data from the DSC Analysis

Material	PVDF				PEEK				COC				POM				PLA	
UVO exposure (min)	0	30	60	120	0	30	60	120	0	30	60	120	0	30	60	120	0	30
First heating																		
T_{g1} (°C)	57	49	50	49	140	139	140	139	a	a	80a	81a					b	b
T_{k1} (°C)					170	169	171	171										
ΔH_{k1} (J/g)					35	32	21*	23*										
T_{m1} (°C)	169	170	169	169	344	345	343	345					176	174	175	175		
ΔH_{m1} (J/g)	48	50	54	54	46	46	50	49					165	178	177	186*		
Cooling																		
T_{gc} (°C)									73	73	73	73					56	52
T_{c1} (°C)	141	141	141	141	308	308	308	308					151	152	151	151		
ΔH_{c1} (J/g)	57	60	59	58	59	59	58	61					186	187	180	173*		
Second heating																		
T_{g2} (°C)					146	146	145	146	80	80	80	81					57	54
T_{m2} (°C)	167	168	168	167	344	344	344	344					176	175	174	174		
ΔH_{m2} (J/g)	58	60	59	58	59	57	59	57					190	186	183	174*		

Indices 1,c,2 indicate first heating, cooling, second heating.
T_m, melting temperature; T_k, crystallization temperature; T_c, cold crystallization temperature; T_g, glass transition temperature; ΔH_m, melting enthalpy; ΔH_k, crystallization enthalpy; ΔH_c, cold crystallization enthalpy.
[a] With differences in enthalpy relaxation processes.
[b] With very sharp enthalpy relaxations (not calculable); error bars: temperature ±1°C, enthalpy ±1.5 J/g.
*Significant changes in the values (indication of thermal aging).

Physical aging is often associated with increase in crack formation or surface roughness. The reduction of polymer weight can lead to reduced Young's moduli and increased brittleness.

Crosslinking, in contrast, can lead to stiffening. The mechanisms leading to increased roughness of the polymer surface are complex. In general, one assumes that a self-limiting process leads to rather well-defined islands. Such roughening is particularly present in plasma treatments, and also seen in UVO treatments. For many polymers including PEEK and PEKK the island size and density can be tailored by the choice of the processing parameters and the exposure time.[19] The selective etching resulting from UVO and plasma treatments of semicrystalline polymers is fascinating, as bands of amorphous and crystalline areas formed during inhomogeneous freezing.[20] The amorphous stripes exhibit lower resistivity to ozone attacks. They are selectively removed in a manner similar to PMMA degrading under deep UV, X-ray, and electron-beam irradiation.[21] These trenches can be further deepened if the strain relief leads to bending of the μC beams. In contrast to UVO, plasma treatments are less sensitive to chain length or crystallinity. The overall effect of UVO treatments is similar to that observed for certain plasma treatments, but the actual mechanisms of the surface chemical changes could differ from polymer to polymer.[22] For some polymers, UVO is less harmful than plasma treatment.[23] Plasma creates fast moving electrons. Ozone does not rely on any electron bombardment. Among others, the nature of the gas, the time of treatment, and the reactor configuration determine the extent of surface modification of polymers in plasma treatment.[24,25] Treatment with oxygen plasma causes oxidation of surface due to ion bombardment and free radicals generated during the treatment.[19,20,24] In addition, plasma removes the polymer layer by ablation.[24]

Figure 4 displays the FTIR data for the aging processes of PVDF, PEEK, POM, COC, and PLA. The UVO treatment has a particularly large impact on COC. One detects an increasing oxidative degradation of the μC's surface. In detail, Figure 4 verifies strong changes for COC with an absorption peak that appears at wavenumbers between 1700 and 1744 cm^{-1} associated with the presence of carbonyl and aldehyde groups resulting from oxidation during UVO exposure. The absorption peaks at 1734 and 1716 cm^{-1} correspond to the presence of C=O or CH=O carbonyl groups, whereas the peak at 3507 cm^{-1} corresponds to the presence of the —OH group. The end aldehydic groups can either be formed by the decomposition of peroxides and hydroperoxides on the polymer surface or by a rearrangement of the peroxy radical intermediate that is formed from chain scission. The peaks between the wavenumbers of 1700 and 1744 cm^{-1} infer that both chain scission and some crosslinking may have occurred on the UVO-treated COC surface. The bands observed in the range from 2944 to 2866 cm^{-1} are for the C—H stretches and the bending modes around 1458 cm^{-1} and also be seen in the untreated COC.[26] For PLA, the ester linkage at the wavenumbers of 1747, 1182, and 1082 cm^{-1} (Figure 4, first column) corresponds to C=O,
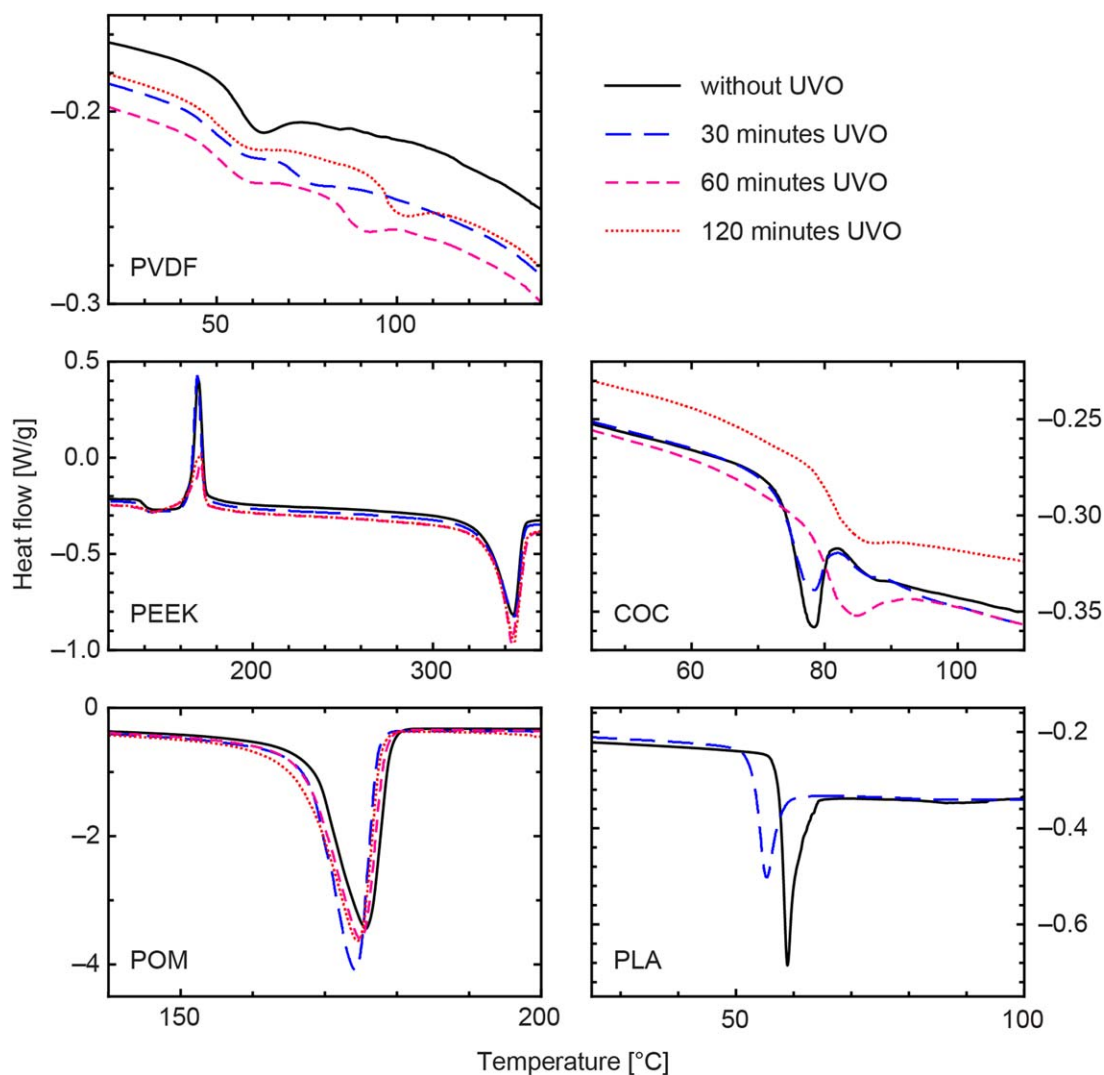
Figure 5. DSC data of PVDF, PEEK, POM, COC, and PLA for the UVO exposure times (0 min, black solid line; 30 min, blue long-dashed line; 60 min, violet dashed line; 120 min, red dotted line) indicated during the first heating from a temperature of 0 to 250°C. These DSC curves allow conclusions on the degree of degradation derived from the temperature-dependent shift in T_g, T_m, and ΔH. [Color figure can be viewed in the online issue, which is available at wileyonlinelibrary.com.]

C—O—C, and O—C—C vibrations.[27] The photo-degradation of PLA is ascertained by the diminished (reduction in the intensity) bands of the ester (1250–1050 cm^{-1}) after 30 min of the UVO exposure (Figure 4, center column). The major peaks characteristic for POM are at wavenumber 903 cm^{-1} associated with the C—O—C symmetric stretch absorption, at wavenumber 1097 cm^{-1} resulting from the C—O—C asymmetric stretch, and at wavenumber 2923 cm^{-1} due to the CH$_2$—O asymmetric stretch. Moderate changes are observed in these peaks of POM after UVO treatment. The decrease in intensity of the ether signals and appearing of strong OH groups around 3600 cm^{-1} (after 120 min) indicate an incipiently chain scission of POM after a period of 120-min UVO treatment. No changes were observed for PVDF and PEEK. The results of FTIR analysis imply that the onset of intolerable degradation is 120 min for POM and 30 min for COC.

Table II and Figures 5–7 display the DSC data of the polymers PVDF, PEEK, POM, COC, and PLA for the first heating, the cooling, and the second heating, respectively. For COC, a reduction in enthalpy relaxation with increasing exposure time can be observed for the first heating (Figure 5) in the glass transition region. This enthalpy relaxation eventually vanishes after the UVO treatment of 120 min (Figure 5). For PVDF and PEEK, one finds slight changes during crystallization and melting. POM shows a broadening of the melting region and an increase of the melting enthalpy (ΔH_m) upon increase in treatment time (Figure 5, Table II). For PLA, T_g-lowering and the accompanying enthalpy relaxation is obvious after the UVO treatment of 30 min. No significant changes were observed during the second heating of the DSC analysis for PVDF, PEEK, and COC as shown in Figure 7. For PLA, a lowering of T_g by 3 K from 57 to 54°C and decreasing enthalpy relaxation indicated a chemical modification. For POM, a decreasing melting
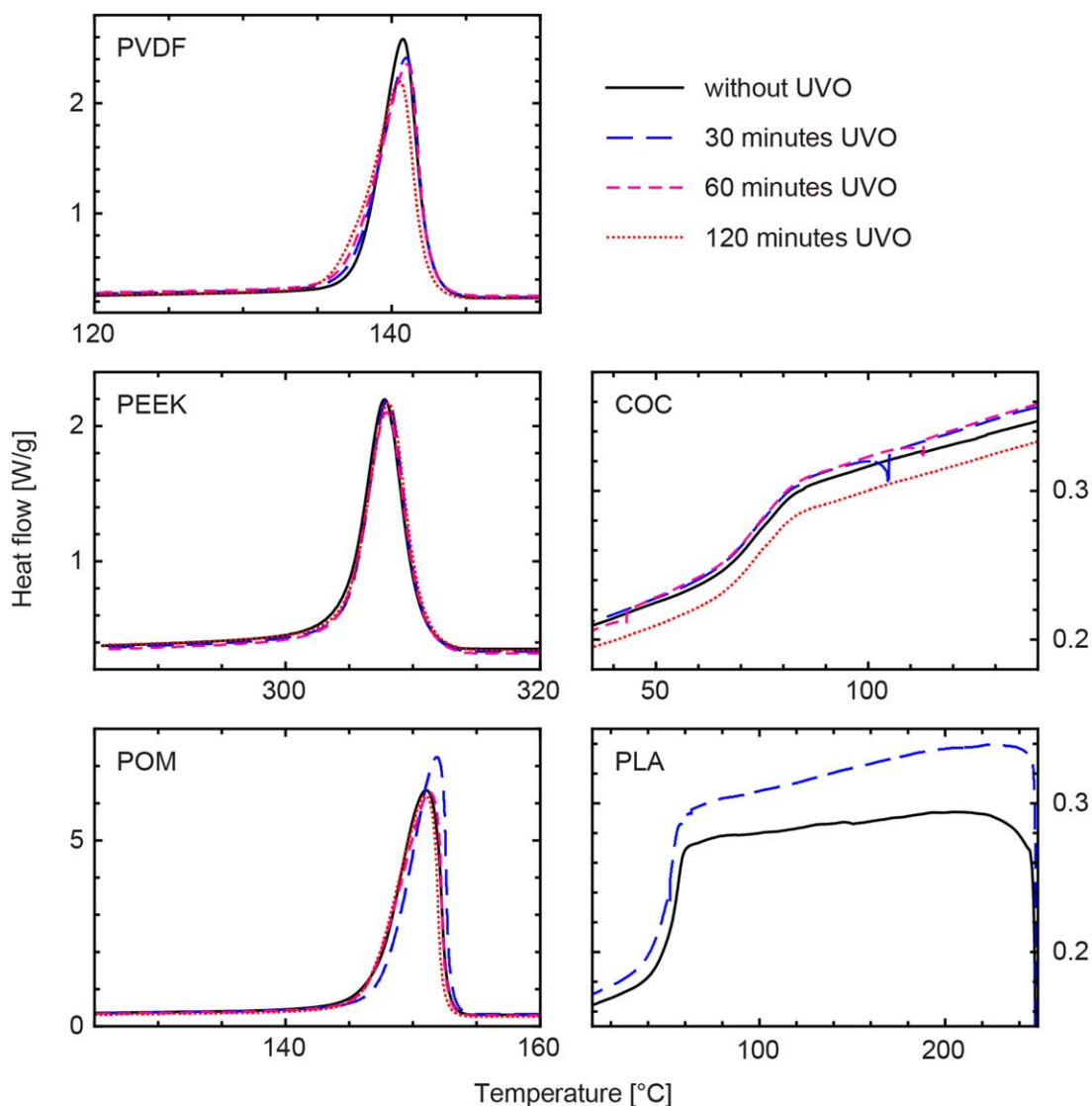
Figure 6. The DSC data of PVDF, PEEK, POM, COC, and PLA for the UVO exposure times (0 min, black solid line; 30 min, blue long-dashed line; 60 min, violet dashed line; 120 min, red dotted line) indicated during the cooling from temperatures of 250 to 0°C show significant changes in the T_g lowering only for PLA. [Color figure can be viewed in the online issue, which is available at wileyonlinelibrary.com.]

temperature (T_m) with increasing exposure time was observed (Figure 7). For PP, this effect is attributed to chemical aging already visible after an UVO exposure of 5 min.[7] As recognized from the data given in Table II for crystalline polymers, it is possible to compare melting (ΔH_m) or crystallization enthalpies (ΔH_k) during cooling and the second heating to identify significant differences in the thermal behavior after irradiation. In case of POM, a clear decrease of melting or crystallization enthalpy as a function of the irradiation time of up to 10% indicates an increasing degradation of the polymer chain.[14] For the other crystalline materials insignificant differences in the enthalpy values were observed. For the amorphous materials incorporated into our study, changes of enthalpy relaxation during or after the glass transition—itself increasing a little with increasing treatment—do show a physical aging, which could be synchronous with a thermal degradation as in the case of COC, see FTIR spectra (Figure 4).

Table III summarizes the experimental results of DSC and FTIR analyses. The onset of severe degradation is deduced examining the shifts in the glass transitions, melting and crystallization regions for the bulk material, and signal changes in the FTIR spectra of the surface. Not only the derived quantities but also the gradual changes of the thermal properties are essential to discern the polymer stability under UVO treatment. In selected cases, the clear changes in DSC, T_g for PLA and COC, T_m and ΔH_m for POM, which indicate chemical and physical aging, correlate to the FTIR spectra (cf. Figure 4). Here, the chemical degradation processes cause polymer damages. In other cases, where no changes were found in the FTIR spectra, distinguishable and rather small changes in the melting enthalpy and glass transition indicate physical aging processes, as seen for the polymer PVDF.

From the experimental results one can deduce the stability of the polymer under UVO treatment. As for the selected five
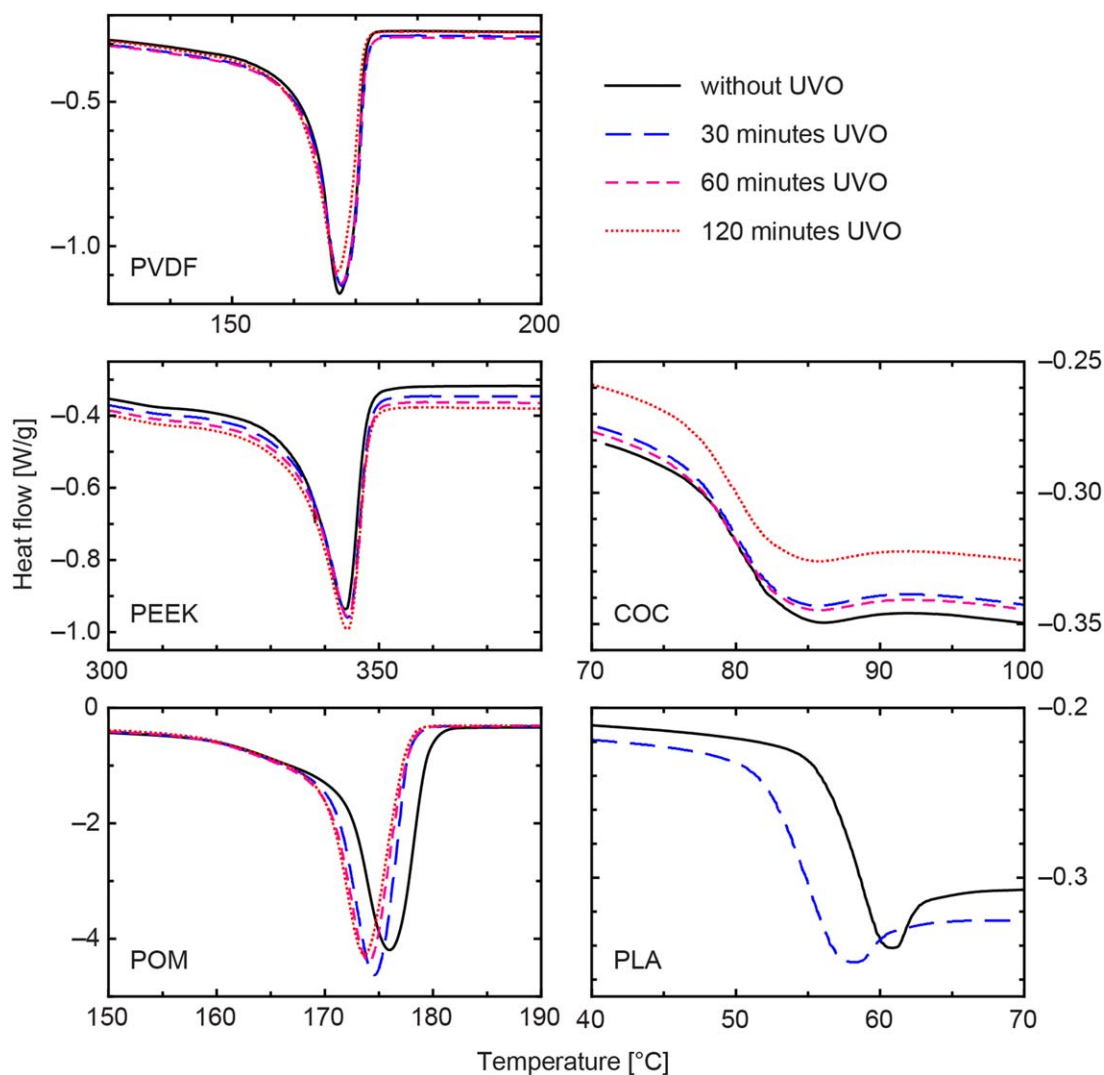
Figure 7. DSC data of PVDF, PEEK, POM, COC, and PLA for the UVO exposure times (0 min, black solid line; 30 min, blue long-dashed line; 60 min, violet dashed line; 120 min, red dotted line) indicated during the second heating from temperatures of 0 to 250°C. The melting behavior of POM and the glass transition temperatures T_g of POM and PLA show a strong UVO treatment dependence. [Color figure can be viewed in the online issue, which is available at wileyonlinelibrary.com.]

Table III. Degradation Effects of UVO Cleaning on Selected Polymer μCs as Analyzed by FTIR and DSC

Material	FTIR	DSC	Stable
		UV–ozone	
PVDF	No changes	Physical aging	Yes
PEEK	No changes	Physical aging	Yes
COC	Thermo-oxidative degradation of the surface	Physical aging	(Yes)
PP	Thermo-oxidative degradation; correlates with treatment time	Clearly physical aging and increasing chemical crosslinking	No
POM	Hydrolytical degradation and others	Clearly increasing physical and chemical aging	No
PLA	Possible changes	Chemical aging	No

Stability within the scope of this study is attributed to polymers without detected chemical aging (DSC) or chemical changes (FTIR). PP data[7] are included for comparison.

polymers only the surface of the μC is affected, the mechanical properties of μC are expected to remain constant within the error bars. This behavior is contrary to PP.[7] Therefore, degradation is usually quantified characterizing the modifications in the surface morphology. The thermal load of the polymer surfaces by UV absorption is particularly detrimental for thermally insulating polymers with low T_g, which excludes PLA from effective UVO cleaning. Therefore, we conclude as rough estimate that apart from PLA a UVO treatment with a duration of 30 min is regarded as acceptable for the other four polymers investigated. This period of time should be considered as maximum.

CONCLUSIONS

Based on the degradation study of 35–50 μm-thin μCs, we conclude that PEEK and PVDF can be UVO cleaned in the conventional fashion. COC is less stable under UVO treatment but exposure times of about 20 min, as proposed for PP, are tolerable. Under the established treatment conditions, the POM and PLA are unstable. The thermal exposure of a few minutes leads to complete failure of the μC beams. Here, UVO or plasma treatments with reduced thermal load could be an option.

REFERENCES

1. McLaughlin, M. C.; Zisman, A. S. The Aqueous Cleaning Handbook: A Guide to Critical-Cleaning Procedures, Techniques, and Validation; AL Technical Communications, LLC: White Plains, NY, 2002.

2. Moisan, M.; Barbeau, J.; Crevier, M.-C.; Pelletier, J.; Philip, N.; Saoudi, B. Pure Appl. Chem. 2002, 74, 349.

3. Moisan, M.; Barbeau, J.; Moreau, S.; Pelletier, J.; Tabrizian, M.; Yahia, L. H. Int. J. Pharm. 2001, 226, 1.

4. Sowell, R. R.; Cuthrell, R. E.; Mattox, D. M.; Bland, R. D. J. Vac. Sci. Technol. 1974, 11, 474.

5. Hook, D. A.; Ohlhausen, J. A.; Krim, J.; Dugger, M. T. J. MEMS 2010, 19, 1292.

6. Urwyler, P.; Schift, H.; Gobrecht, J.; Häfeli, O.; Altana, M.; Battiston, F.; Müller, B. Sens. Actuators A: Phys. 2011, 172, 2.

7. Urwyler, P.; Pascual, A.; Kristiansen, P. M.; Gobrecht, J.; Müller, B.; Schift, H. J. Appl. Polym. Sci. 2013, 127, 2363.

8. Vig, J. R. J. Vac. Sci. Technol. A 1985, 3, 1027.

9. Köser, J.; Gaiser, S.; Müller, B. Eur. Cells Mater. 2011, 21, 479.

10. Bhattacharyya, A.; Klapperich, C. M. Lab Chip 2007, 7, 876.

11. Zhao, X.; Urwyler, P.; Müller, B. Eur. Cells Mater. 2012, 23, 40.

12. Urwyler, P.; Häfeli, O.; Schift, H.; Gobrecht, J.; Battiston, F.; Muller, B. Proc. Eng. 2010, 5, 347.

13. Zhou, Q.; Xanthos, M. Polym. Degrad. Stab. 2009, 94, 327.

14. Ehrenstein, G. W.; Pongratz, S. Beständigkeit von Kunststoffen; Carl Hanser Verlag: Munich, 2007.

15. Kusy, R. P.; Whitley, J. Q. Am. J. Orthodont. Dentofac. Orthop. 2005, 127, 420.

16. Eve, S.; Mohr, J. Proc. Eng. 2009, 1, 237.

17. Nie, H.-Y.; Walzak, M. J.; Berno, B.; McIntrye, N. S. Appl. Surf. Sci. 1999, 144-145, 627.

18. Zweifel, H. Stabilization of Polymeric Materials; Springer Verlag: Berlin, 1997.

19. Urwyler, P.; Zhao, X.; Pascual, A.; Schift, H.; Müller, B. Eur. J. Nanomed. 2014, 6, 37.

20. Althaus, J.; Urwyler, P.; Padeste, C.; Heuberger, R.; Deyhle, H.; Schift, H.; Gobrecht, J.; Pieles, U.; Scharnweber, D.; Peters, K.; Müller, B. Proc. SPIE 2012, 8339, 83390Q.

21. Moore, J. A.; Choi, J. O. ACS Symp. Ser. 1991, 475, 156.

22. Ebnesajjad, S. Handbook of Adhesives and Surface Preparation: Technology, Applications and Manufacturing; William Andrew Publishing (Elsevier): Norwich, 2010.

23. Berdichevsky, Y.; Khandurina, J.; Guttman, A.; Lo, Y.-H. Sens. Actuators B 2004, 97, 402.

24. Torregrosa-Coque, R.; Martín-Martínez, J. M. Plasma Process. Polym. 2011, 8, 1080.

25. Chang, C. Y.; Sze, S. M. ULSI Technology; McGraw-Hill: New York, 1996.

26. Yang, T. C. K.; Lin, S. S. Y.; Chuang, T. H. Polym. Degrad. Stab. 2002, 78, 525.

27. Zhanga, J.; Satoa, H.; Tsujib, H.; Nodac, I.; Ozakia, Y. J. Mol. Struct. 2005, 735-736, 249.